11th International Conference on Marine Technology
MARTEC 2018

CFD ANALYSIS ON UNSTEADY YAW MOTION CHARACTERISTIC OF A TOWED SHIP

Nur Adlina Aldin[2], Ahmad Fitriadhy[1*], Nurul Aqilah Mansor[2], and Adi Maimun[3]

[1]Programme of Maritime Technology, School of Ocean Engineering,
Universiti Malaysia Terengganu,, 21030 Kuala Terengganu, Terengganu

[2]Postgraduate Students, Programme of Maritime Technology, School of Ocean Engineering,
Universiti Malaysia Terengganu, 21030 Kuala Terengganu, Terengganu

[3] Marine Technology Center (MTC), Faculty of Mechanical Engineering,
Universiti Teknologi Malaysia, Malaysia

ABSTRACT

Instability of a ship towing system indicated by vigorous yaw motion of a towed ship may reduce the safety of the navigation especially in the restricted with heavy congestion waterways. To stabilise this towing system, a comprehensive investigation on a towline configuration is therefore required. This paper presents Computational Fluid Dynamic (CFD) approach to analyse the unsteady yaw motion characteristic of a towed ship using symmetrical bridle towline. Several towing parameters such as various towline length and towing's velocity have been taken into account. Here, a towed ship designates as 1B (barge) is employed in the simulations. The results revealed that the subsequent increase of towline length will degraded barge course stability due to increment of her lateral motion by 13.69%. However, longer towline will decrease the towline tension by 1.38%. The increment of towing's velocity from V_s=0.509 m/s to 0.653 m/s, reduce barge course stability indicated by increased yaw motion of 10.77% meanwhile her slewing period decreased by 0.2%.

Keywords : *Yaw motion, CFD, towing point, towline length, and course stability.*

1.0 INTRODUCTION

The drastic growth of shipping activities leads to heavy congestion due to abundant of ships in the waterways that threaten the safety navigation of a towed ship. If the towing stability of a towed vessel is not secure, it can cause monetary losses due to delayed arrival and marine accidents due to large irregular behavior [1]. Therefore, an extensive yaw motion investigation is then required to observe behavior of towed barge using symmetrical bridle towline during the operations.

In recent years, researchers have presented numerous studies on investigating the unsteady yaw motion of towed vessel [2-7]. Inoue et al. (1979), Lee (1989), Kijima et al. (1990), Fitriadhy et al. (2011), and Fitriadhy et al. (2016) analysed the towed vessel unsteady yaw motion by means of analytical analysis. Mathematical prediction method estimating yaw moment was useful to compare the different types of vessel, however, only according trim conditions [8, 9]. Lee (1989) studied the yaw moment of the barge using different materials of towline which are polyester and nylon [10] while effect of different towline length, tow point location on the barge and tug is proposed by Fitriadhy et al. (2011) [2] and

*Corresponding author: naoe.afit@gmail.com

number of nodes of towline and effect of skegs to the oscillation of yaw motion [7]. Experimental approach was conducted by Im et al. (2015), Zan et al. (2012) and You et al. (2015) to investigate the effect of different towline configuration [11] and employing active thruster [1]. Im et al. (2015) performed experiment to study the influence of skeg to the yaw motion and extending the research by using Computational Fluid Dynamics (CFD) for further validation.

Since numerical calculation and experiment have limitation in accurately reflecting the effect of interference and viscosity that affect the motion of vessel, CFD is employed to analyze the effects of nonlinearities, such as generation of 3D vortices [12]; computed the sway force and yaw moment during drift and steady yaw motion and analysed the flow field around the barge. Nonaka et al. (1986) determine the fluid motion around the hull of a vessel and the hydrodynamics force exerted on a drifting vessel as well as presence of strong nonlinearities and complex flowfield [13]. CFD approach had been widely applied in maritime technology field such as estimating the vessel performance [14-16], resistance [17-21], and ship motions characteristics [22-27].

Thus, this paper presents a CFD simulation to predict the unsteady yaw motion characteristics of towed barge (1B). Here, a commercial CFD so called Flow3D v11.2 is utilized by applying unsteady Reynolds-Averaged Navier Stokes Equation (RANSE). Flow3D incorporates different technique (TruVOF) to capture the free surface and computes flow variable only within one fluid. This major quality of Flow3D reduces computational time significantly.

2.0 GOVERNING EQUATION

The CFD flow solver on FLOW-3D version 10.1 is based on the incompressible unsteady RANS equations in which the solver applies the Volume of Fluid (VOF) to track the free surface elevation. The interface between fluid and solid boundaries is simulated with the fractional area volume obstacle representation favor method. This method computes open area and volume in each cell to define the area that is occupied by obstacle.

2.1 Continuity and Momentum Equation

The continuity and momentum equations for a moving object and the relative transport equation for VOF function are

$$\frac{V_f}{\rho}\frac{\partial \rho}{\partial t} + \frac{1}{\rho}\nabla.\left(\rho \vec{u} A_f\right) = -\frac{\partial V_f}{\partial t} \tag{1}$$

$$\frac{\partial \vec{u}}{\partial t} + \frac{1}{V_f}\left(\vec{u}A_f.\nabla\vec{u}\right) = -\frac{1}{\rho}\left[\nabla_\rho + \nabla.\left(\tau A_f\right)\right] + \vec{G} \tag{2}$$

$$\frac{\partial F}{\partial t} + \frac{1}{V_f}\nabla.\left(F\vec{u}A_f\right) = -\frac{F}{V_f}\frac{\partial V_f}{\partial t} \tag{3}$$

where ρ is the density of the fluid, $\vec{u}$ is the fluid velocity, V_f is the volume fraction,A_f is the area fraction, p is the pressure, τ is the viscous stress tensor, G denotes gravity and F is the fluid fraction.

In the case of coupled GMO's motion, Eqs.(1) and (2) are solved at each time step and the location of all moving objects is recorded and the area and volume fractions updated using the FAVOR technique. Equations (3) are solved with the source term $\left(-\frac{\partial V_f}{\partial t}\right)$ on the right-hand side which is computed as

$$-\frac{\partial V_f}{\partial t} = \vec{U}_{obj}\vec{n}S_{obj}/\,V_{cell} \tag{4}$$

where S_{obj} is the surface area, $\vec{n}$surface normal vector, $\vec{U}_{obj}$ is the velocity of the moving object at a mesh cell and V_{cell} is the total volume of the cell [28].

2.2 Turbulence Model

The RNG turbulence model was used for the simulation of the exchange flow between open water and floating object since it accounts for low Reynolds number effects [29-31]. Applying the double averaging strategy to the transport equations for TKE and its dissipation rate produces the turbulence model for the flow. The resulting equations are:

$$\frac{\delta k}{\delta t} + U_j \frac{\delta k}{\delta x_j} = \frac{\delta}{\delta x_j}\left[\left(v + \frac{v_t}{\sigma_k}\right)\frac{\delta k}{\delta x_j}\right] + P_k + B_k + W_k - \varepsilon \quad (5)$$

$$\frac{\delta \varepsilon}{\delta t} + U_j \frac{\delta \varepsilon}{\delta x_j} = \frac{\delta}{\delta x_j}\left[\left(v + \frac{v_t}{\sigma_\varepsilon}\right)\frac{\delta \varepsilon}{\delta x_j}\right] + C_{1\varepsilon}\frac{\varepsilon}{k}(P_k + B_k)(1 + C_{3\varepsilon}R_f) + W_\varepsilon - C_{2\varepsilon}^{*}\frac{\varepsilon^2}{k} \quad (6)$$

$$P_k = v_t S^2 = v_t\left(\frac{\delta U_i}{\delta x_j} + \frac{\delta U_j}{\delta x_i}\right)\frac{\delta U_i}{\delta x_j} \quad (7)$$

$$B_k = \beta g_i \frac{v_t}{\sigma_s}\frac{\delta s}{\delta x_i} \quad (8)$$

where P_k is the shear production term of TKE, $S = \sqrt{2S_{ij}S_{ji}}$ is the modulus of the mean rate of strain tensor and $S_{ij} = \frac{1}{2}\left(\frac{\delta U_i}{\delta x_j} + \frac{\delta U_j}{\delta x_i}\right)$, B_k is the buoyant production term of TKE, W_k is the wake production tern of TKE, W_ε is the wake production term in ε, σ_k and σ_ε are the turbulent Prandtl numbers for k and ε, and $C_{i\varepsilon}$, $C_{3\varepsilon}$ and $C_{2\varepsilon}^{*}$ are model coefficients.

2.3 Body Motion Computation

The body motion was analysed in a space-fixed Cartesian coordinate system, the global coordinate system. The governing equation of the six degree of freedom (DOF) of a rigid body motion can be expressed in this coordinate system as

$$\frac{d}{dt}(m\vec{v}_c) = \vec{f} \quad (9)$$

$$\frac{d}{dt}(M_c.\vec{w}_c) = \vec{m}_c \quad (10)$$

The index C denotes the centre of mass of the body, m denotes the mass of the body, $\vec{v}_c$ the velocity vector, M_c is the tensor of the moments of inertia, $\vec{\omega}_c$ is the angular velocity vector, $\vec{f}$ denotes the resulting force vector and $\vec{m}_c$ denotes the resultant moment vector acting on the body [12]. The resultant force $\vec{f}$ has three components; surface force, field forces and external forces:

$$\vec{f} = \int_S (T - \rho I).\vec{n}dS + \int_V \rho_b \vec{b}dV + \vec{f}E \quad (11)$$

Here, $\rho_b$is the density of the body. The only field force considered is the gravity, so the volume integral of above equation (right hand side) reduces to $m\vec{g}$, where g is the gravity acceleration vector. The vector $f\vec{E}$ denotes the external forces acting in the body. [32]

3.0 SIMULATION CONDITIONS

3.1 Principal Data of Ship

The principal dimensions barge (1B) are presented in Table 1. Her respective body plan is shown in Figure 1.

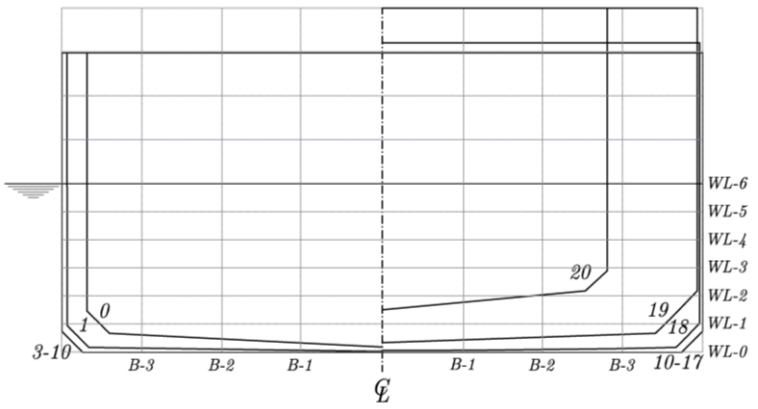

Figure 1: Body plan of barge.

Table 1. Principal dimensions of barge (1B).

Description	1B	
	Full-scale	Model
Length, *L(m)*	60.96	1.219
Breadth, *B(m)*	10.67	0.213
Draft, *d(m)*	2.74	0.0548
Volume, $V(m^3)$	1646.2	0.01317
L/B	5.71	5.71
Block coefficient,C_b	0.92	0.92
k_{yy2}/L	0.3266	0.3266
$X_{G\ abaft\ the\ midship}$,$(m)$	-1.04	-0.0208

3.2 Parametric Studies

Table 2 shows various of towline length, l' used in the simulation. Towing's velocity, V_s and towing point location, l_b' used in the simulation is kept constant by , V_s=0.509 m/s and l_b'=0.5, respectively. The tug is replaced with a sphere which inhibits similar characteristics of tug. Various towing's velocity, V_s is shown in Table 3 while towing point location is set to l_b'=0.5 and towline length, l'=1.0 L.

Table 2: Various towline length, l'

Towline length, l'	Towing velocity, V_s $(\frac{m}{s})$
1.0 L	0.509
2.0 L	
3.0 L	

Table 3: Various towing velocity, V_s

Towline length, l'	Towing velocity, V_s $(\frac{m}{s})$
1.0 L	0.509
	0.582
	0.653

3.3 Computational Domain and Boundary Conditions

The computational domain uses a structured mesh that is defined in a Cartesian. Referring to Figure 2, the boundary condition is mark in the mesh block. The boundary condition at X-max boundary is specified velocity so that there is flow of water. In order to save computational time, velocity is assigned to water at X-max boundary. As for X-min, Y-max and Y-min boundary, outflow is assigned to prevent reflection while Z-min is symmetry and Z-max is specified pressure. The boundary conditions for this simulation are shown in Table 4.

Table 4: Boundary condition

Boundary	Conditions
X_{min}	Specified velocity
X_{max}	Outflow
Y_{min}	Outflow
Y_{max}	Outflow
Z_{min}	Symmetry
Z_{max}	Specified pressure

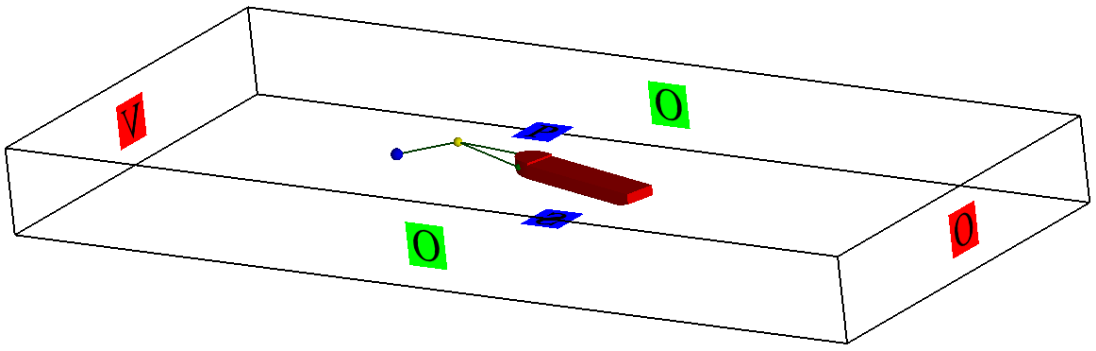

Figure 2: Boundary conditions

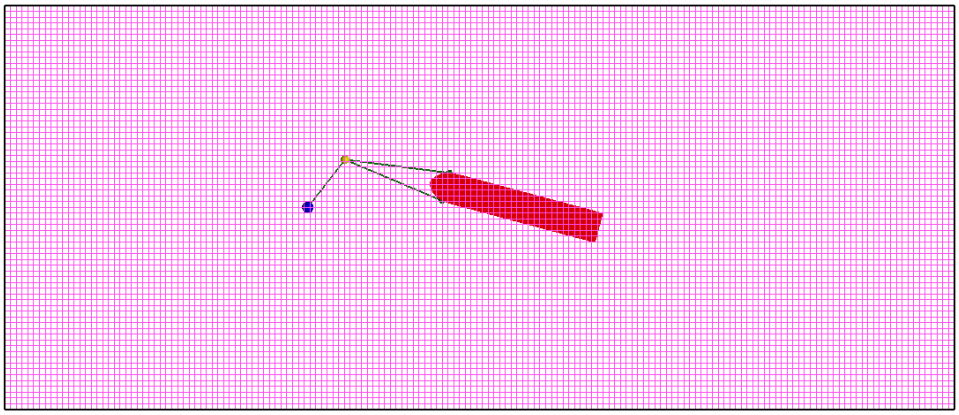

Figure 3: Meshing generation

The meshing generation is created in Flow3D v11.2 as shown in Figure 3. The barge is coupled through a towline. A virtual tug, a sphere model is assigned prescribed motion while barge as towed ship was set as coupled motion in X-translational, Y-translational and Z-rotational motions (surge, sway and yaw motions). The barge was in 15° inclination arrangement initially. The towline is set as massless rope with spring coefficient of $0.787 N/m^2$.

Based on the applications of Flow3D v11.2, the average duration of every simulation was about 70-80 hours (4 parallel computations) on a HP Z820 workstation PC with processor Intel (R) Xeon (R) CPU ES-2690 v2 @ 3.00 GHz (2 processors) associated with the installed memory (RAM) of 32.0 GB and 64-bit Operating System.

3.4 Mesh Independent Study

Mesh independent study is necessary for examining the adequate number of mesh in order to ensure the accuracy of computation results. Table 5 shows the result of the mesh independent study. The total numbers of cells about 995,841 in case C is then selected from all the cases with the reasonable accuracy of CFD solution associated with less computational time. Table 5 shows the mesh independent study of the system; towline length, l'=1.0 L, towing's point location on barge, l'_b=0.5 and towing's velocity, Vs =0.509 in calm water while Figure 4 shows different yaw motion for different number of cells.

Table 5: Mesh Independent Study

Case	Total number of real cells	Maximum yaw motion (rad/s)
A	503 880	0.3002
B	743 850	0.3006
C	995 841	0.2682
D	1 258 008	0.2537

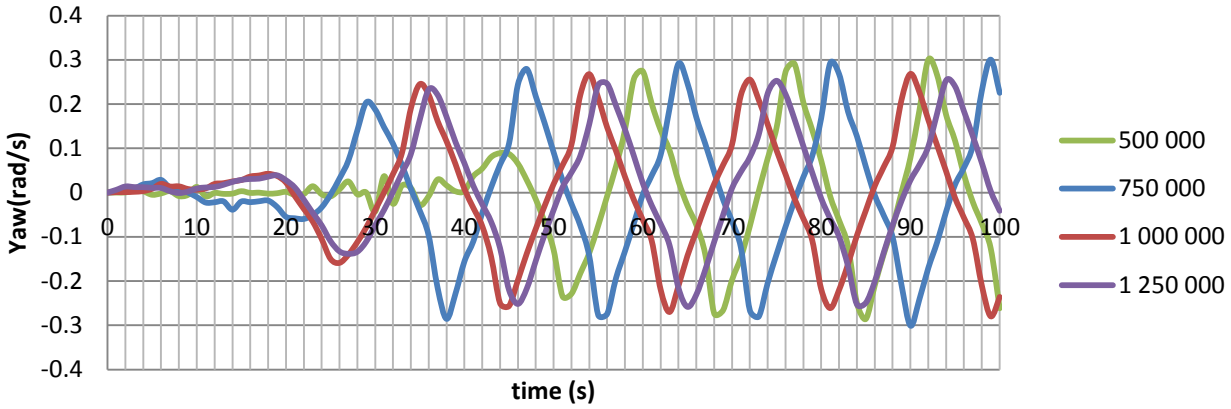

Figure 4: Mesh independent study

4.0 RESULTS AND DISCUSSIONS

Figures 5 – 8 show the CFD simulations have been successfully carried out to predict the course stability of the towing system in the various towline length and towing's velocity. The simulations results of sway and yaw motions of the barge associated with the towline tension are discussed.

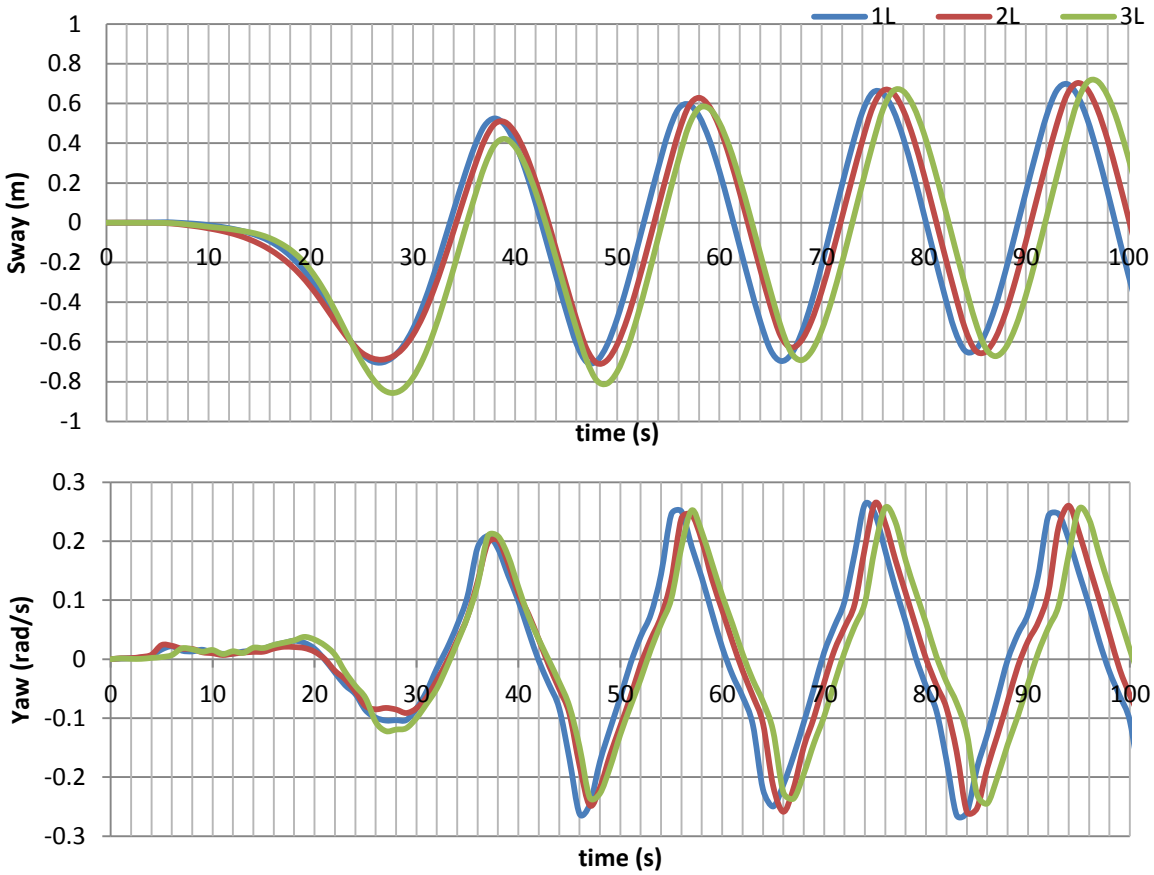

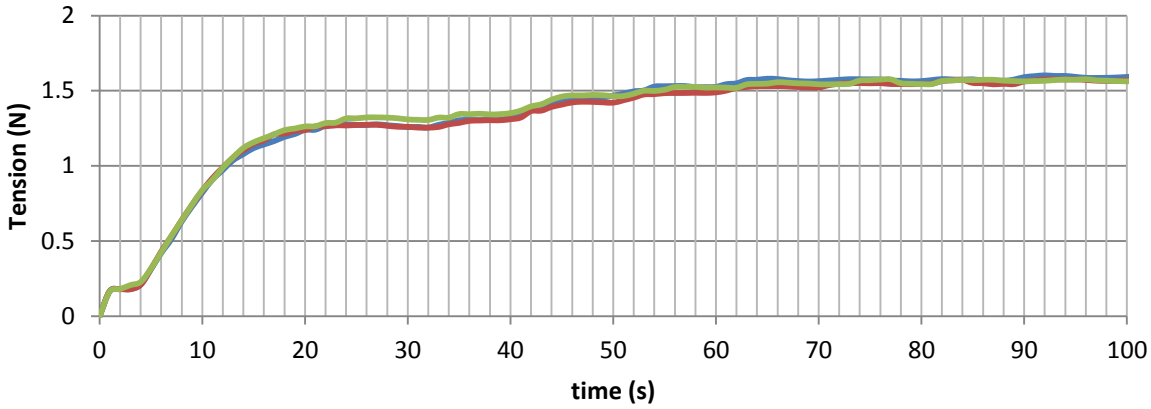

Figure 5: Characteristics of sway and yaw motion of 1B associated with the towline tension at various towing point location

The characteristics of sway and yaw motion in various towline length is displayed in Figure 5. Extending towline length from l^{ι}=1.0 to 2.0 and 3.0 resulted in the significant increment of sway motion by 2.96% and 1.04%, respectively. The fishtailing period of 1B was lowered by 11.76% as towline length increased from l^{ι}=1.0 to 3.0. It was noted that yaw motion decreased 4.39% as the towline length is increased from l^{ι}=1.0 to 3.0. The course stability of 1B was degraded as increasing towline length increased sway motion of barge. Based on numerical approach conducted by Fitriadhy et al. (2017) [33], their findings show that the lateral motion was increased as the towline length was extended from l^{ι}=1.0 to l^{ι}=3.0. The towline tension is appeared to be insignificant as the towline length increased as agreed by Fitriadhy and Yasukawa (2011)[2].

As shown by Figure 8, the visualization of free surface elevation showed that l^{ι}=3.0 shows vigorous sway motion compared to l^{ι}=2.0 and l^{ι}=1.0. Higher pressure indicated by red color is present at bow of the barge while blue color showed lower pressureHowever, the higher pressure (red color) is obviously seen around the hull at l'=2.0 L. The suction at the portside affects the lateral force and yaw moment of the barge [12]. It is due to high pressure is exerted on the hull at the port side and cause greater pressure difference to the starboard side which influence the oscillation of yaw and sway motion.

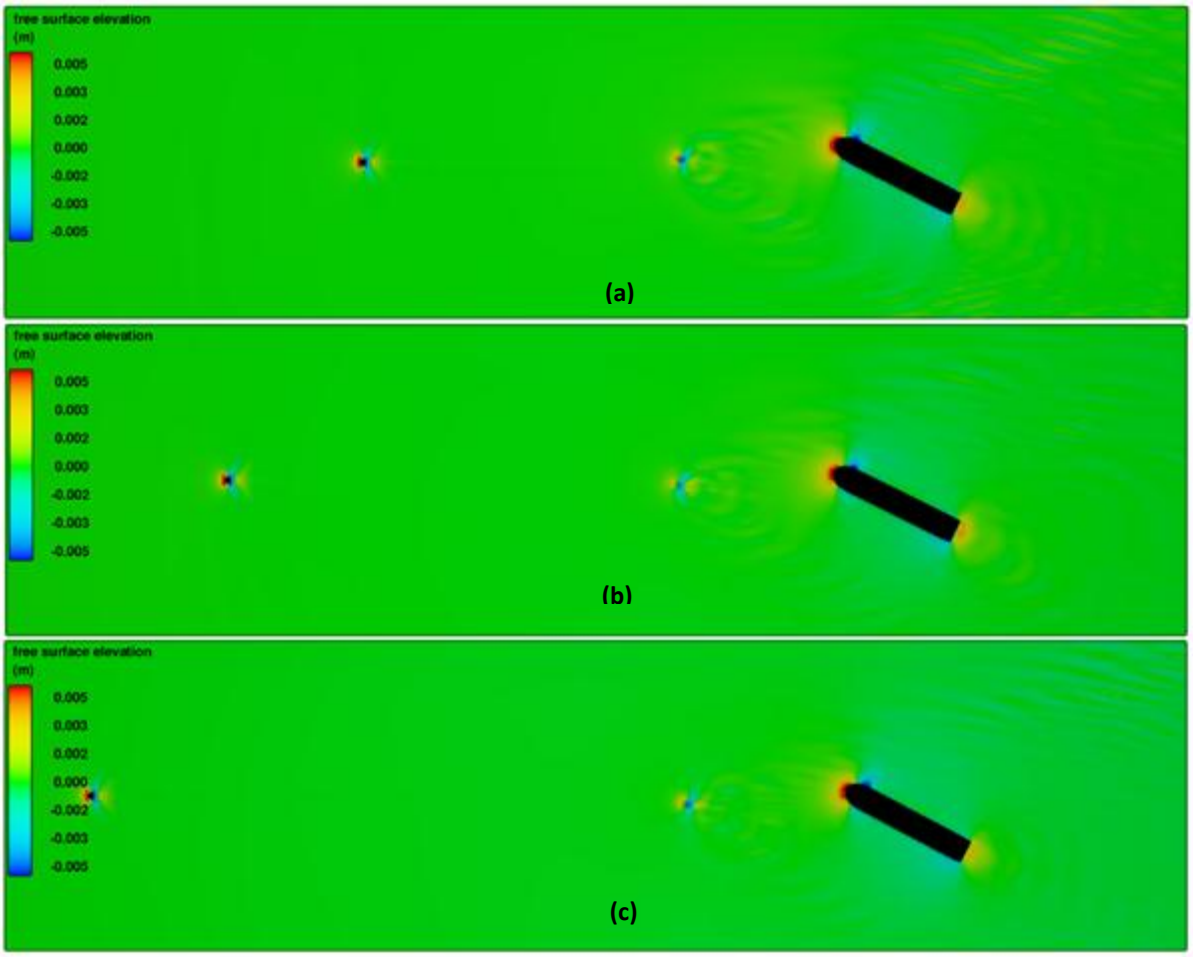

Figure 6: Free surface elevation, Vs= 0.509, l' = 1.0 L (a), 2.0 L (b), and 3.0 L (c)

4.2 Effect of Towing's velocity

Figure 7 shows the characteristics of sway and yaw motion associated with dynamic towline tension in various towing's velocity. The subsequent increased of towing's velocity from Vs= 0.509 m/s to 0.653 m/s resulted in increment of sway motion by 13.69%. The yaw motion of the barge increased by 9.43% and 1.48% as towing's velocity increased from Vs=0.509 to 0.582 m/s and Vs=0.582 to 0.653 m/s, respectively. Reduction of slewing period by 16.67% is resulted due to increasing towing's velocity. Higher wave crest (red colour) present at the bow region and prone to increase as the velocity increased from Vs=0.509 m/s to 0.653 m/s which proportional to high pressure as shown in Figure 8. Increasing pressure giving rise to higher resistance as stated by Zou and Larsson (2013)[34]. As the speed is low, the water escapes the narrow channel between the hull and goes below and around the hulls. The negative pressure gradients leads to higher suction forces, thus increased the yaw moment tothe hull. Thus, it is proven that the higher pressure at both bow and stern of the barge resulted in highest yaw moment of the barge when Vs=0.653 m/s compared to 0.509 m/s and 0.582 m/s.

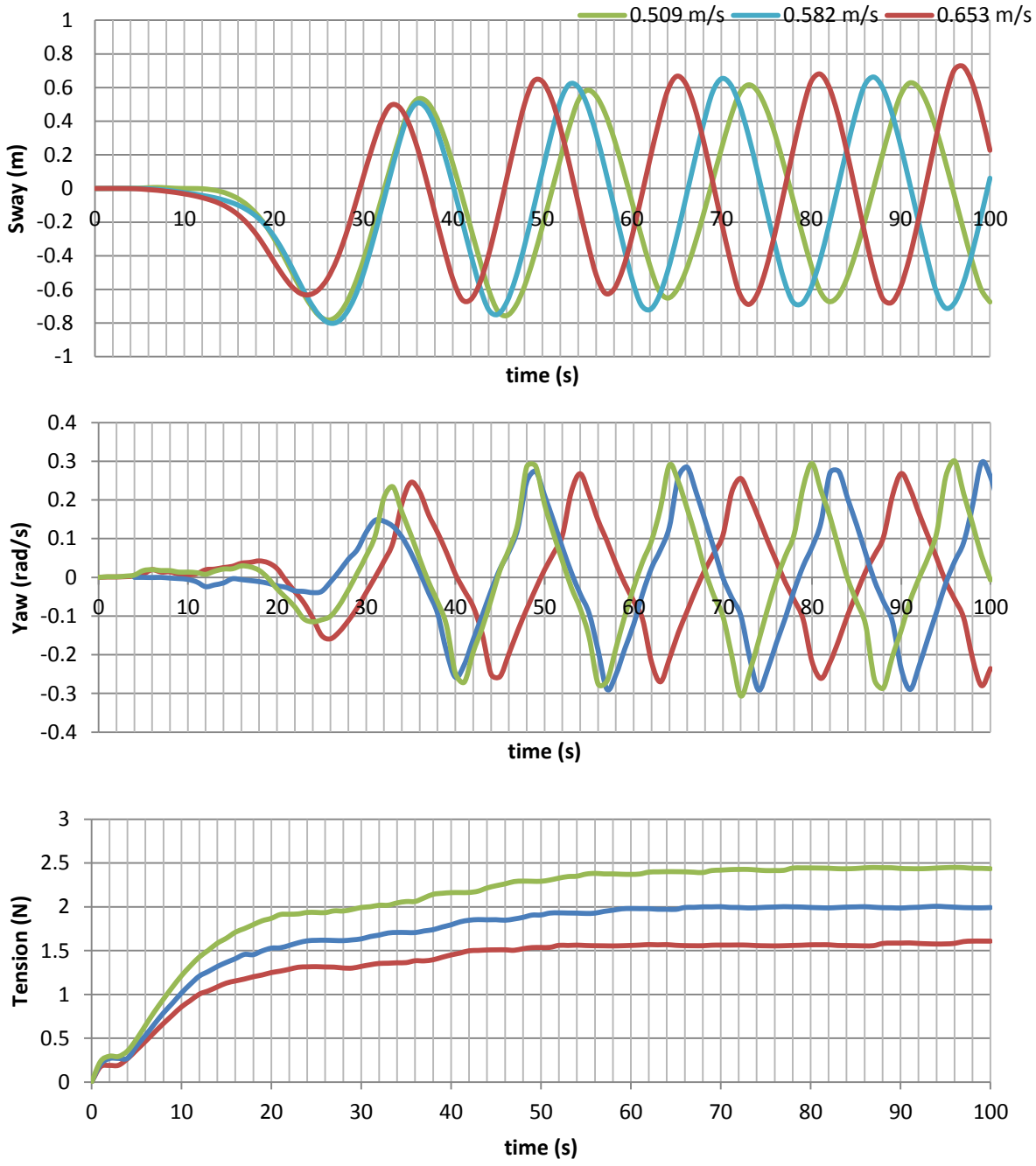

Figure 7: Characteristics of sway and yaw motion of 1B associated with towline tension in various towline lengths

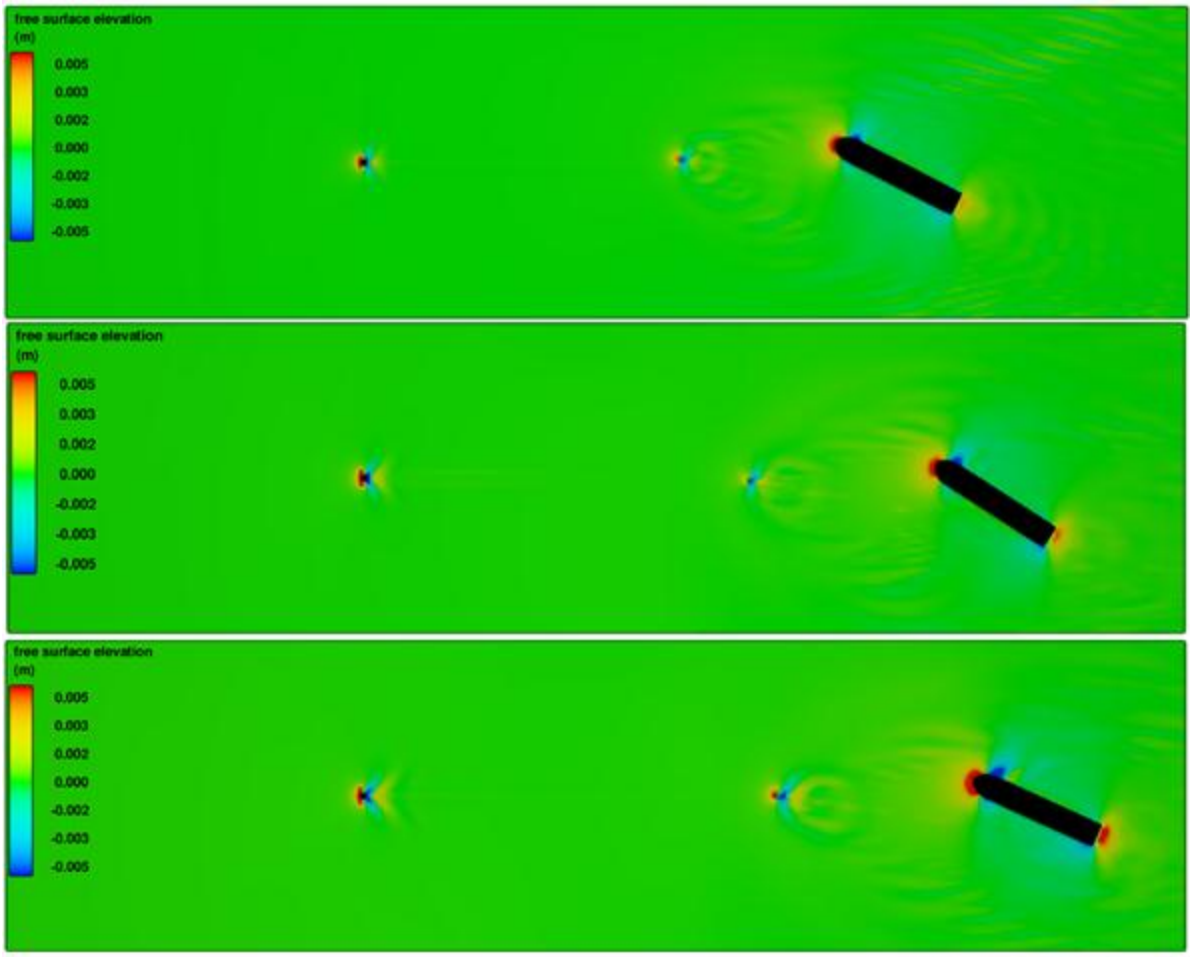

Figure 8: Free surface elevation, Vs = (a) 0.509, (b) 0.582, and 0.653 m/s.

5.0 CONCLUSION

The Computational Fluid Dynamics (CFD) analysis on the course stability of the ship's towing system was successfully performed using FLOW3D version 11.2 software. The effects of different towline length and towing's velocity wereinvestigated. The simulation results are as follows:

- Extending towline length, l' from 1.0 to 3.0 was degrading course stability of the barge indicated by increment of sway and yaw motion. However, the towline tension decreased by 1.38%.
- The increase of towing's velocity from V_s = 0.509 m/s to 0.653 m/s increased the yaw motion by 10.77%. Meanwhile, the towline tension increased by 19.81% and 18.10% as towing's velocity increased from V_s = 0.509 m/s to 0.582 m/s and V_s = 0.653 m/s, respectively.

ACKNOWLEDGEMENTS

The authors greatly appreciate to Ministry Higher Education of Malaysia for the financial support awarded from Fundamental Research Grant Scheme (FRGS) VOT NO 59414.

NOMENCLATURE

CFD	Computational Fluid Dynamic
1B	Barge

l'	Ratio of towline length with respect to length of barge
l'_b	Ratio of towing point location with respect to barge length
V_s	Tug's velocity
RANSE	Reynolds-Averaged Navier Stokes Equation

REFERENCE

1. You, Y.J., Hur, J. and Jung, J. (2015). *An Experimental Study on an Auxiliary Towing System for an FPSO using Active Thrusters*. Applied Ocean Research, 52, 62-72.

2. Fitriadhy, A. and Yasukawa, H. (2011). *Course Stability of a Ship Towing System*. Ship Technology Research, 58(1), 4-23.

3. Fitriadhy, A. and Yasukawa, H. (2011). *Turning Ability of a Ship Towing System*. Ship Technology Research, 58(2), 112-124.

4. Fitriadhy, A., Yasukawa, H. and Koh, K. (2013). *Course Stability of a Ship Towing System in Wind*. Ocean Engineering, 64, 135-145.

5. Fitriadhy, A., Yasukawa, H., Yoneda, T., Koh, K. and Maimun, A. (2014). *Analysis of an asymmetrical bridle towline model to stabilise towing performance of a towed ship*. Jurnal Teknologi (Sciences & Engineering), 66(2), 151-156.

6. Fitriadhy, A., Yasukawa, H. and Maimun, A. (2015). *Theoretical and Experimental Analysis of a Slack Towline Motion on Tug-towed Ship during Turning*. Ocean Engineering, 99, 95-106.

7. Fitriadhy, A., Yasukawa, H., Wan Nik, W.B. and Abu Bakar, A. (2016). *Numerical Simulation of Predicting Dynamic Towline Tension on a Towed Marine Vehicle*. International Conference on Ships and Offshore Structures ICSOS 2016 31 August - 2 September 2016, Hamburg, Germany.

8. Inoue, S., Hirano, M. and Mukai, K. (1979). *The Nonlinear Terms of Lateral Force and Moment Acting on Ship Hull in the Case of Manoeuvering*. Trans. West-Japan Soc. Nav. Archit(58).

9. Kijima, K., Katsuno, T., Nakiri, Y. and Furukawa, Y. (1990). *On the manoeuvring performance of a ship with theparameter of loading condition*. Journal of the Society of Naval Architects of Japan, 1990(168), 141-148.

10. Lee, M.-L. (1989). *Dynamic Stability of Nonlinear Barge-towing System*. Applied mathematical modelling, 13(12), 693-701.

11. Zan, U.I., Yasukawa, H., Koh, K.K. and Fitriadhy, A. (2012). *Model Experimental Study of a Towed Ship's Motion*. The 6th Asia-Pacific Workshop on Marine Hydrodymics-APHydro.

12. Im, N., Lee, S. and Lee, C. (2015). *The influence of skegs on course stability of a barge with a different configuration*. Ocean Engineering, 97, 165-174.

13. Nonaka, K., Fuwa, T. and Nimura, T. (1986). *Measurement of wake flow and hydrodynamic force distribution on a ship model with drift angle (2nd report, Tanker model)*. J. Soc. Naval Architects of West Japan, 72, 197-212.

14. van Oers, B. and Toxopeus, S. (2006). *On the relation between flow behaviour and the lateral force distribution acting on a ship in oblique motion*. 10th International Cooperation on Marine Engineering Systems ICMES, London, UK.

15. Miyazaki, H., Ueno, M. and Tsukada, Y. *Numerical study about effects of stern skeg on course stability*. in *The Twenty-first International Offshore and Polar Engineering Conference*. 2011. International Society of Offshore and Polar Engineers.

16. Broglia, R., Dubbioso, G., Durante, D. and Di Mascio, A. (2013). *Simulation of turning circle by CFD: Analysis of different propeller models and their effect on manoeuvring prediction*. Applied Ocean Research, 39, 1-10.

17. Tezdogan, T., Demirel, Y.K., Kellett, P., Khorasanchi, M., Incecik, A. and Turan, O. (2015). *Full-scale Unsteady RANS CFD Simulations of Ship Behaviour and Performance in Head Seas due to Slow Steaming*. Ocean Engineering, 97, 186-206.

18. Maki, K.J., Broglia, R., Doctors, L.J. and Di Mascio, A. (2013). *Numerical investigation of the components of calm-water resistance of a surface-effect ship*. Ocean Engineering, 72, 375-385.

19. Fitriadhy, A., Jamaluddin, A., Norsani, W.M., Wan Nik, W.B., Bakar, A., Azlan, M. and W. M. Noor, C. (2014). *Frictional Resistance's Prediction of a Trimaran Ship in Calm Water using Computational Fluid Dynamic (CFD) Approach*.

20. Fitriadhy, A., Lim, P.S. and Jamaluddin, A., *CFD Investigation on Total Resistance Coefficient of Symmetrical and Staggered Catamaran Configurations through Quantifying Existence of an Interference Factor*, in *The First International Conference on Ships and Offshore Structures ICSOS 2016*. 2016: Hamburg, Germany. p. 1-20.

21. Fitriadhy, A., Azmi, S., Mansor, N.A. and Aldin, N.A. (2017). *Computational fluid dynamics investigation on total resistance coefficient of a high-speed" deep-V" catamaran in shallow water*. International Journal of Automotive and Mechanical Engineering, 14, 4369-4382.

22. Tezdogan, T., Incecik, A. and Turan, O. (2016). *A Numerical Investigation of the Squat and Resistance of Ships Advancing through a Canal using CFD*. Journal of marine science and technology, 21(1), 86-101.

23. Sadat-Hosseini, H., Kim, D.-H., Carrica, P.M., Rhee, S.H. and Stern, F. (2016). *URANS simulations for a flooded ship in calm water and regular beam waves*. Ocean Engineering, 120, 318-330.

24. Cercos-Pita, J.L., Bulian, G., Pérez-Rojas, L. and Francescutto, A. (2016). *Coupled simulation of nonlinear ship motions and a free surface tank*. Ocean Engineering, 120, 281-288.

25. Zhang, G., Zhang, X. and Pang, H. (2015). *Multi-innovation auto-constructed least squares identification for 4 DOF ship manoeuvring modelling with full-scale trial data*. ISA transactions, 58, 186-195.

26. Fitriadhy, A. and Adam, N.A. (2017). *Heave and pitch motions performance of a monotricat ship in head-seas*. International Journal of Automotive and Mechanical Engineering, 14, 4243-4258.

27. Fitriadhy, A., Razali, N. and AqilahMansor, N. (2017). *Seakeeping performance of a rounded hull catamaran in waves using CFD approach*. Journal of Mechanical Engineering and Sciences, 11(2), 2601-2614.

28. *FLOW-3D 10.1.1 User Manual*. (2013). Flow Science Inc.

29. Yakhot, V. and Orszag, S.A. (1986). *Renormalization group analysis of turbulence. I. Basic theory*. Journal of scientific computing, 1(1), 3-51.

30. Yakhot, A., Rakib, S. and Flannery, W. (1994). *Low-Reynolds number approximation for turbulent eddy viscosity*. Journal of scientific computing, 9(3), 283-292.

31. Koutsourakis, N., Bartzis, J.G. and Markatos, N.C. (2012). *Evaluation of Reynolds stress, k-ε and RNG k-ε turbulence models in street canyon flows using various experimental datasets*. Environmental fluid mechanics, 1-25.

32. Yan, S. and Huang, G. (1996). *Dynamic Performance of Towing System-Simulation and Model Experiment*. Proceedings, OCEAN, 96.

33. Fitriadhy, A., Aswad, M., Aldin, N.A., Mansor, N.A., Bakar, A. and Nik, W. (2017). *Computational fluid dynamics analysis on the course stability of a towed ship*. Journal of Mechanical Engineering and Sciences, 11(3), 2919-2929.

34. Zou, L. and Larsson, L. (2013). *Numerical predictions of ship-to-ship interaction in shallow water*. Ocean Engineering, 72, 386-402.